Journal of the Optical Society of Korea
Vol. 13, No. 3, September 2009, pp. 398-402

DOI: 10.3807/JOSK.2009.13.3.398

Terahertz Frequency Spreading Filter via One-dimensional Dielectric Multilayer Structures

Minwoo Yi[1], Youngchan Kim[1,2], Dae-Su Yee[2], and Jaewook Ahn[1]*

[1]*Department of Physics, Korea Advanced Institute of Science and Technology, Daejeon 305-701, Korea*

[2]*Center for Safety Measurement, Korea Research Institute of Standards and Science, Daejeon 305-340, Korea*

(Received July 3, 2009 : revised August 13, 2009 : accepted August 14, 2009)

We present a method of using one-dimensional dielectric multilayer structures for designing terahertz frequency spreading filters. The interference of terahertz pulses in these structures composed of alternating weak and strong refractive materials allows design of well-separated THz frequency components within a modulation-limited THz spectral envelope. The design characteristics of these coarse THz combs are limited by the saturation effect and also by the deformation of the THz pulse time-traveling within the structure. The details of the designed THz waveform synthesis from these THz multilayer spectral filters are verified by experiments using time-domain terahertz pulsed spectroscopy.

Keywords: Terahertz, Multilayer, Interference filters

OCIS codes: (300.6495) Spectroscopy, terahertz; (350.2460) Filters, interference; (230.4170) Multilayers; (350.4600) Optical engineering; (300.6500) Spectroscopy, time-resolved

I. INTRODUCTION

The scientific and technological interest in the electromagnetic waves in the newly available frequency range of 0.1∼10 THz, or terahertz (THz) waves, for short, has been gradually increasing, because of the potential uses of THz waves in a large variety of up-and-coming applications [1]. Among the recent discoveries in THz science and technology, one can easily find many future applications in communications, material characterizations, biological and medical imaging, and precision spectroscopy of molecules [2]. Also, along with the commercial development of femtosecond lasers, THz time-domain spectroscopy (THz-TDS) has been widely adopted, in particular, for the measurement of absorption and dispersion of materials in the THz frequency range [3-7]. However, a THz pulse is extremely broadband in frequency and its usage beyond simple spectroscopy and imaging can be also easily found in its applications, especially with THz waves in designed waveforms. The ability to generate THz radiation with a variety of temporal and spectral shapes is indeed essential for many advanced applications: THz indoor communications [8], THz active imaging [9], quantum devices [10], and even quantum computing [11].

There have been many attempts in synthesizing complex THz waveforms [12-16], and one of the most common wave-manipulating devices is a spectral pass filter. THz filters can be categorized into two types, according to the changeability of THz frequency and/or intensity via external stimuli: active or passive filters. Recent progress in dynamically and actively switchable THz metamaterial filters has demonstrated their potentials in future THz applications

[16-18]. Active THz filters provide more fertile changeability in frequency and/or energy manipulation, but at the expense of complexity and cost. Passive filters, on the other hand, are less complicated and cost-effective though hardly adjustable. Several experiments have been attempted to get specially intended passive THz filters. These filter designs are all based on currently available design approaches for optical devices: photonic bandgap crystals [19, 20], perforated metal sheets [21, 22], interference in a multilayer structure [15, 23], and so on.

*Corresponding author: jwahn@kaist.ac.kr

Conventional interference frequency filters, structures with multilayer stacks of materials, have an advantage of making the design process easier and more systematic. By alternating layers of THz transparent materials with proper dielectric properties, plentiful THz waveforms can be easily realizable [24, 25]. THz multilayer interference structures have been made in a number of different configurations and materials which are easily and widely available. Furthermore, the structure made of material with no absorption could be applied either as a filter or a mirror, as the transmittance and reflectance functions are complementary. The fabricated structures are operated as mirrors for short-range or indoor THz communication [26, 27].

In this paper, we design and characterize terahertz frequency spreading filters which are one-dimensional dielectric multilayer structures composed of alternating materials with high and low index of refraction. This THz frequency spreading filter can be explained in that the degree of THz pulse broadening decreases with the number of periods increases. Conventional transmission configuration of THz-TDS is utilized to investigate the dielectric properties of the structures designed for a spectral filter.

II. DESIGN OF MULTILAYER INTERFERENCE FILTERS

1. The basic theory of transmission in multilayer structures

In general, the wave transmission through a one-dimensional dielectric structure can be formulated using a transfer matrix method [28]. First, we decompose the wave transmission through the structures into several suitable blocks of calculation steps. Each block can be described in terms of a matrix. According to the transfer matrix formalism, a homogeneous non-absorbing dielectric layer with constants of ε and μ can be expressed by a 2×2 matrix,

$$M=\begin{bmatrix} m_{11} & m_{12} \\ m_{21} & m_{22} \end{bmatrix}=\begin{bmatrix} \cos\delta & \frac{i}{\beta}\sin\delta \\ i\beta\sin\delta & \cos\delta \end{bmatrix}, \quad (1)$$

where we set $\delta=2\pi ndcos\theta/\lambda_0$ and $\beta=\sqrt{\varepsilon/\mu}\,cos\theta\,(=\sqrt{\mu/\varepsilon}\cos\theta)$ for TE (TM) polarization, respectively. Also θ and d denote the incident angle and the thickness of the layer, respectively.

The product of all the individual transfer matrices is equal to the transfer matrix of an entire structure. An analytical model of an entire multilayer structure of n periods consisting of high/low index material layer can be expressed as

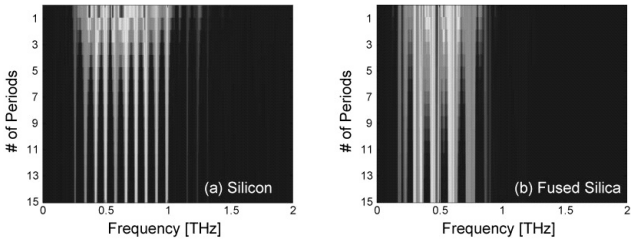

FIG. 1. Calculated THz spectra image for (a) 500-㎛ silicon / 100-㎛ air and (b) 500-㎛ fused silica / 100-㎛ air periods when the number of periods is discretely changed. The width of interferometric THz component initially decreases, and almost reaches a saturated bandwidth.

$$M_{entire}=(M_H M_L)^n=\begin{bmatrix} M_{11} & M_{12} \\ M_{21} & M_{22} \end{bmatrix}. \quad (2)$$

When a normally incident plane-wave propagates through this one-dimensional interference structures, we can calculate the reflection and transmission coefficient of multilayer interference structures from the method of transfer formalism. The reflectance and transmittance functions, $R(\lambda_0)$ and $T(\lambda_0)$, of the entire structure in free space are calculated from the elements of total transfer matrix given as:

$$R(\lambda_0)=\left|\frac{M_{11}+M_{12}-M_{21}-M_{22}}{M_{11}+M_{12}+M_{21}+M_{22}}\right|^2, \quad T(\lambda_0)=\left|\frac{2}{M_{11}+M_{12}+M_{21}+M_{22}}\right|^2 \quad (3)$$

2. Design of THz frequency spreading filter

Now we consider a THz pulse traveling through a dielectric layer. This pulse bounces back and forth within a layer. At a condition of constructive interference, higher transmittance occurs for the given spectral component. In contrast, if destructive interference occurs lower transmittance is made. This interference effect has accumulated by increasing the number of high and low index periods. In proportion to the number of periods, the width of each frequency component initially decreases, and reaches a saturated bandwidth. There will be some equally distributed THz frequency components like interferometric frequency components in the THz spectra. The main characteristic of these THz spectra are attributed to THz pulses bouncing back and forth via multilayer structures. For adjustable quality of equally distributed THz frequency components via one-dimensional multilayer structures, we discontinuously change the number of periods. Figure 1 shows calculated THz spectra images when the number of periods is changed for 500-㎛-thick silicon or fused silica wafer with an 100-㎛-thick air gap. The width of interferometric THz component initially decreases, and reaches a saturated bandwidth as shown in Fig. 1.

III. EXPERIMENTAL PROCEDURE

In the experiments, we used an 80-MHz Ti:sapphire laser, which delivered 30-fs laser pulses with a broadband IR spectrum centered at 810 nm. The optical excitation pulses of 250-mW laser power are illuminated at a large-area interdigitated THz emitter [29] that was biased with V_{pp} = 20 V of 63-kHz square wave AC voltage. The generated THz pulses were collected and then refocused with four 90° off-axis parabolic mirrors. The electro-optic effect in a (110) ZnTe crystal of 1-mm thickness is used for the detection of THz pulses [30]. The angle between the probe and THz polarization was optimized to maximize the detected THz field [31].

Commonly, multilayer interference filters are composed of a high and low refractive index material. In the work reported here, silicon and fused silica wafers are selected as high refractive index materials because of their low dispersion and absorption for the THz region. Intrinsic high-resistivity float-zone (FZ) silicon has a constant refractive index and is lossless for THz frequencies [3, 4]. Undoped silicon Wafer used in our work has a resistivity of > 1.0 kΩcm, an orientation of (100), and a thickness of 500 ㎛ and is polished on both sides. With silicon wafer, 500-㎛-thick and double-side-polished fused silica wafer is used. Fused silica is a good THz material because of relatively low refractive index and optical isotropy, and is easily available and of economical choice. The optical properties of fused silica have been reported in the THz region [3]. The low index material is air, which has a unity refractive index and no birefringence.

The structures constituted by silicon or fused silica wafers interchanging with air gaps, are created in open frames. High and low index layers are easily alternated front and back, using an adjustable frame. The dielectric material layers are gripped by an aluminum block. The incident area of the interference structure is open and wide enough, so that THz pulse can penetrate through without edge diffraction.

IV. RESULTS AND DISCUSSION

Figures 2 and 3 show, respectively, a set of measured (blue line) and calculated (red line) THz time-domain signals and spectra from various periods of silicon/air and fused silica/air layers from n = 0 to 10. Here, n means the number of periods, composed of high and low refractive index dielectric layers. One-dimensional THz multilayer structures used for the study are fabricated by varying the number of periods. Each period is layered using a 500-㎛-thick silicon or fused silica wafer with an 100-㎛-thick air gap. Measured and calculated THz temporal shapes and spectra are rearranged for clarity in Figs. 2 and 3.

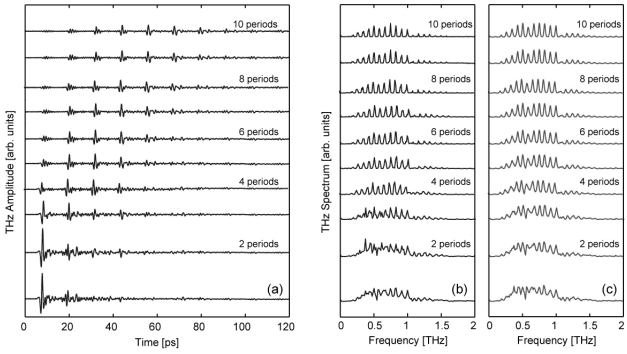

FIG. 2. A set of measured THz temporal shapes (a) and spectra (b), and calculated THz spectra (c) from different periods of 500 ㎛ silicon and 100 ㎛ air layers.

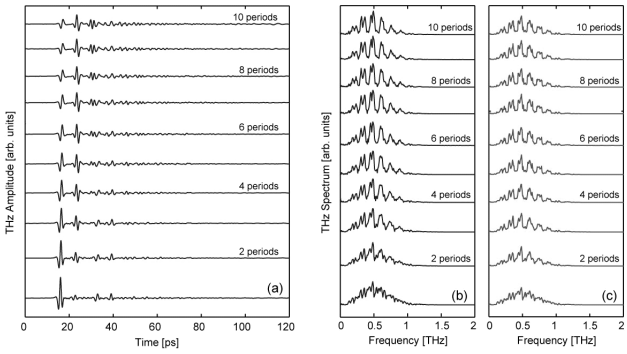

FIG. 3. A set of measured THz temporal shapes (a) and spectra (b), and calculated THz spectra (c) from different periods of 500 ㎛ fused silica and 100 ㎛ air layers.

Some THz frequency components like interferometric frequency components have appeared in the THz spectra. In proportion to the numbers of periods, the width of each frequency components initially decreases, and has almost reached a saturated bandwidth. These complicated THz spectra are attributed to THz pulses commuting back and forth via multilayer structures.

As shown in both experimental and calculated spectral data, the amplitude of THz frequency components around intervals of ~0.083 THz (=~83 GHz) for silicon/air layer and 0.140 THz (=~140 GHz) for fused silica/air layer decreases due to destructive interference, as the number of periods increases. These intervals are related with time difference between transmitted pulse and one cycle time-delayed pulse inside a period of high/low index layer. There are 12 and 7.2 ps time difference between 0th and 1st internally reflected in 500 ㎛ silicon/100 ㎛ air and 500 ㎛ fused silica/100 ㎛ air layers. These time intervals accurately match inverse of frequency component intervals. Finally, THz spectra composed of equally-distributed interferometric patterns have appeared as shown in Fig. 2 and 3 as the effect of destructive interference has accumulated.

We explain that this THz spreading filter is based on the fact that the gain in the width of the envelope of THz temporal pulses has slowed as shown in Fig. 4. Increasing the number of periods, the overall shape of THz time-domain trace is firstly much broader than THz pulse without multilayer structures because of the effect of THz signals traveling multi-pass inside dielectric layers. However, the degree of pulse broadening comparatively dwindles because some time delayed and multiple reflected THz pulses are positioned at the same time.

To confirm the degree of envelope of THz time traces broadening, we fit Gaussian pulses on the measured THz temporal shapes. All measured THz temporal shapes are fitted by Gaussian pulses like as shown in the inset of Fig. 4. Inset shows measured THz time signal and fitted Gaussian pulse for 8 silicon/air periods. A maximum of THz time-trace is picked as the center of fitted Gaussian function. We extract the full width at the half maximum bandwidth (FWHM) of fitted Gaussian pulses for the different number of periods to discuss that equally-distributed THz frequency components in modulation-limited THz spectra are related with the envelope of THz temporal pulses. The bandwidths of fitted Gaussian pulses for the different number of periods are shown in Fig. 4. In the Figure, measured data for silicon/air and fused silica/air layers are marked as open marks, and calculated results are also plotted as solid lines, for the comparison. All lines, calculation results, are described by an equation of broadening THz pulse:

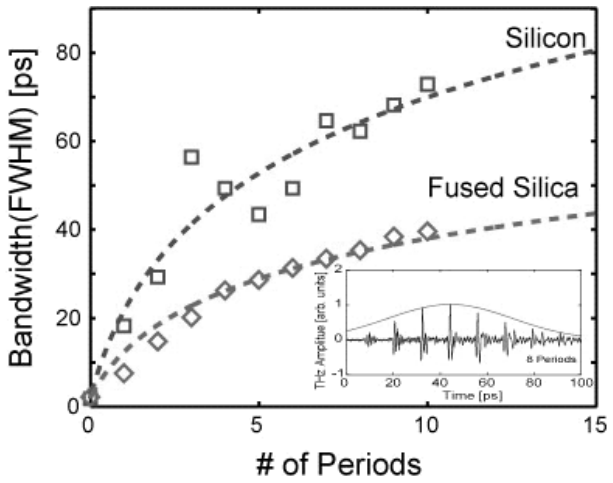

FIG. 4. Bandwidths of fitted Gaussian pulses for different number of periods. Measured (open marks) and calculated data (solid lines) for silicon/air and fused silica/air periods are plotted for the comparison. Inset, measured THz temporal shape and fitted Gaussian pulse for 8 silicon/air periods. A maximum of THz time-trace is picked as the center of fitted Gaussian function.

$$FWHM = \alpha \ln(n+1) + \tau_0, \quad (4)$$

where γ is a broadening coefficient empirically obtained from the relation of $\alpha=\gamma(d_0/c)-\tau_0$. Here, d_0 is an optical length of one high/low index dielectric period and τ_0 is measured FWHM of fitted Gaussian pulse without structure. Parameter γ are 5.02 and 4.74 for silicon/air and fused silica/air, respectively. n is the number of periods and one period is summed to be valid for the case of no multilayer structure. Figure 4 shows that the degree of widening envelope of THz time-domain signal does not proportionally increase. We can perceive that the bandwidth of interferometric THz components via multilayer structures has almost reached the critical bandwidth as shown in Fig. 1. Because the refractive index of silicon is larger than that of fused silica, THz waveforms traveling via silicon/air structures are much broader, slowly saturated and larger γ. This study helps to make equally spreading THz frequency components and a set of multilayer structures could be employed for calibrating the linearity of THz amplitude/power measurements. The knowledge of spectral analysis of THz pulses may improve the understanding and fabrication of THz multilayer structures.

V. CONCLUSION

In this study, we have designed and characterized THz frequency spreading filters constructed as one-dimensional dielectric multilayer structures of alternating weak and strong refractive materials. When the number of high and low index periods increases, the width of interferometric THz components initially decreases and then reaches a saturated bandwidth. These interferometric THz components are equally distributed within a modulation-limited THz spectral envelope. Each THz component has an interval of as much as the inverse of the time difference between the two adjacent pulses internally reflected in a stack layer. These THz frequency components are coarse frequency combs in modulation-limited THz spectrum with the saturation of the envelope of THz time-shapes. The details of the designed THz waveform synthesis from these THz multilayer spectral filters are verified by experiments using time-domain terahertz pulsed spectroscopy.

ACKNOWLEDGMENT

This work was supported by the IT R&D program of MKE/IITA [2008-F-021-01, Development of high speed terahertz/NIR spectroscopic endoscopy using THz frequency comb technology].

REFERENCES

1. M. Tonouchi, "Cutting-edge terahertz technology," Nat. Photonics **1**, 97-105 (2007).
2. D. Mittleman, *Sensing with Terahertz Radiation* (Springer-Verlag, Berlin, Germany, 2003).
3. D. Grischkowsky, S. Keiding, M. van Exter, and C. Fattinger, "Far-infrared time-domain spectroscopy with terahertz beams of dielectrics and semiconductors," J. Opt. Soc. Am. B **7**, 2006-2015 (1990).
4. J. Dai, J. Zhang, W. Zhang, and D. Grischkowsky, "Terahertz time-domain spectroscopy characterization of the far-infrared absorption and index of refraction of high-resistivity float-zone silicon," J. Opt. Soc. Am. B **21**, 1379-1386 (2004).
5. D. M. Mittleman, R. H. Jacobsen, R. Neelamani, R. G. Baraniuk, and M. C. Nuss, "Gas sensing using terahertz time-domain spectroscopy," Appl. Phys. B: Lasers and Optics **67**, 379-390 (1998).
6. J. Hlinka, T. Ostapchuk, D. Nuzhnyy, J. Petzelt, P. Kuzel, C. Kadlec, P. Vanek, I. Ponomareva, and L. Bellaiche, "Coexistence of the phonon and relaxation soft modes in the terahertz dielectric response of tetragonal $BaTiO_3$," Phys. Rev. Lett. **101**, 167402-1~167402-4 (2008).
7. Y. He, P. I. Ku, J. R. Knab, J. Y. Chen, and A. G. Markelz, "Protein dynamical transition does not require protein structure," Phys. Rev. Lett. **101**, 178103-1~178103-4 (2008).
8. I. A. Ibraheem, N. Krumbholz, D. Mittleman, and M. Koch, "Low dispersive dielectric mirrors for future terahertz wireless communication systems," IEEE Microwave and Wireless Components Letters **18**, 67-69 (2008).
9. W. L. Chan, K. Charan, D. Takhar, K. F. Kelly, R. G. Baraniuk, and D. M. Mittleman, "A single pixel terahertz imaging system based on compressed sensing," Appl. Phys. Lett. **93**, 121105-1~121105-3 (2008).
10. B. E. Cole, J. B. Willams, B. T. King, M. S. Sherwin, and C. R. Stanley, "Coherent manipulation of semiconductor quantum bits with terahertz radiation," Nature (London) **410**, 60-63 (2001).
11. J. Ahn, D. N. Hutchinson, C. Rangan, and P. H. Buchsbaum, "Quantum phase retrieval of a rydberg wave packet using a half-cycle pulse," Phys. Rev. Lett. **86**, 1179-1182 (2001).
12. J. Ahn, A. Efimov, R. Averitt, and A. Taylor, "Terahertz waveform synthesis via optical rectification of shaped ultrafast laser pulses," Opt. Exp. **11**, 2486-2496 (2003).
13. N. E. Yu, C. Kang, H. K. Yoo, C. Jung, Y. L. Lee, C.-S. Kee, D.-K. Ko, and J. Lee, "Temperature dependent terahertz generation at periodically poled stoichiometric lithium tantalate crystal using femtosecond laser pulses," J. Opt. Soc. Korea **12**, 200-204 (2008).
14. M. Yi, K. H. Lee, I. Maeng, J.-H. Son, R. D. Averitt, and J. Ahn, "Tailoring the spectra of terahertz emission from CdTe and ZnTe electro-optic crystals," Jpn. J. Appl. Phys. **47**, 202-204 (2008).
15. W. Withayachumnankul, B. M. Fischer, and D. Abbott, "Quarter-wavelength multilayer interference filter for terahertz waves," Opt. Comm. **281**, 2374-2379 (2008).
16. H.-T. Chen, W. J. Padilla, J. M. O. Zide, A. C. Gossard, A. J. Taylor, and R. D. Averitt, "Active terahertz metamaterial devices," Nature (London) **444**, 597-600 (2006).
17. H.-T. Chen, J. F. O'Hara, A. K. Azad, A. J. Taylor, R. D. Averitt, D. B. Shrekenhamer, and W. J. Padilla, "Experimental demonstration of frequency-agile terahertz metamaterials," Nat. Photonics **2**, 295-298 (2008).
18. T. Driscoll, S. Palit, M. M. Qazilbash, M. Brehm, F. Keilmann, B.-G. Chae, S.-J. Yun, H.-T. Kim, S. Y. Cho, N. M. Jokerst, D. R. Smith, and D. N. Basov, "Dynamic tuning of an infrared hybrid-metamaterial resonance using vanadium dioxide," Appl. Phys. Lett. **93**, 024101-1~024101-3 (2008).
19. E. Özbay, E. Michel, G. Tuttle, R. Biswas, K. M. Ho, J. Bostak, and D. M. Bloom, "Double-etch geometry for millimeter-wave photonic band-gap crystals," Appl. Phys. Lett. **65**, 1617-1619 (1994).
20. H. Kurt and D. S. Citrin, "Photonic crystals for biochemical sensing in the terahertz region," Appl. Phys. Lett. **87**, 041108-1~041108-3 (2005).
21. T. Matsui, A. Agrawal, A. Nahata, and Z. V. Vardeny, "Transmission resonances through quasicrystal arrays of subwavelength apertures," Nature (London) **446**, 517-521 (2007).
22. C. Kang, C.-S. Kee, I.-B. Sohn, and J. Lee, "Spectral properties of THz-periodic metallic structures," J. Opt. Soc. Korea **12**, 196-199 (2008).
23. N. Matsumoto, T. Nakagawa, K. Kageyama, N. Wada, and Y. Sakabe, "Terahertz band-pass filter fabricated by multilayer ceramic technology," Jpn. J. Appl. Phys. **45**, 7499-7502 (2006).
24. H. Němec, P. Kužel, F. Garet, and L. Duvillaret, "Time-domain terahertz study of defect formation in one-dimensional photonic crystals," Appl. Opt. **43**, 1965-1970 (2004).
25. I. Hosako, "Multilayer optical thin films for use at terahertz frequencies: method of fabrication," Appl. Opt. **44**, 3769-3773 (2005).
26. N. Krumbholz, K. Gerlach, F. Rutz, M. Koch, R. Piesiewicz, T. Kürner, and D. Mittleman, "Omnidirectional terahertz mirrors: a key element for future terahertz communication systems," Appl. Phys. Lett. **88**, 202905-1~202905-3 (2006).
27. C. Jansen, S. Wietzke, V. Astley, D. M. Mittleman, and M. Koch, "Fully flexible terahertz bragg reflectors based on titania loaded polymers," in Proc. *Conference on Quantum Electronics and Laser Science Conference on Lasers and Electro-optics, (CLEO/QELS)* (San Jose, California, USA, 2008), art. no. 4551728.
28. E. Hecht, *Optics*, fourth ed. (Addison-Wesley, San Francisco, USA, 2002).
29. A. Dreyhaupt, S. Winnerl, T. Dekorsy, and M. Helm, "High-intensity THz radiation from a microstructured large-area photoconductor," Appl. Phys. Lett. **86**, 121114-1~121114-3 (2005).
30. Q. Wu and X.-C. Zhang, "Ultrafast electro-optic field sensors," Appl. Phys. Lett. **68**, 1604-1606 (1996).
31. P. Planken, N. Nienhuys, H. J. Bakker, and W. T. Wenckebach, "Measurement and calculation of the orientation dependence of terahertz pulse detection in ZnTe," J. Opt. Soc. Am. B **18**, 313-317 (2001).